Appendix A. Supplementary data

Predicted THz-wave absorption property in all-inorganic perovskite, $CsPbI_3$ thin film: Integrity at the grain boundary

Inhee Maeng[1,+], Si Chen[2,+], Seungjun Lee[3,+,†], Shenghao Wang[2,*] Young-Kyun Kwon[3,4*], and Min-Cherl Jung[5,*]

[1]*YUHS-KRIBB, Medical Convergence Research Institute, College of Medicine, Yonsei University, Seoul, 03722, Republic of Korea*

[2]*Materials Genome Institute, Shanghai University, Shanghai, 200444, China*

[3]*Department of Physics, Kyung Hee University, Seoul, 02447, Republic of Korea*

[4]*Department of Information Display and Research Institute for Basic Sciences, Kyung Hee University, Seoul, 02447, Republic of Korea.*

[5]*Division of Materials Science, Faculty of Pure and Applied Sciences, University of Tsukuba, Ibaraki, 305-8577, Japan*

[+]These authors contributed equally: Inhee Maeng, Si Chen, and Seungjun Lee

[†]Present address: Department of Electrical and Computer Engineering, University of Minnesota, Minneapolis, Minnesota 55455, USA

[*]Correspondence: Shenghao Wang (shenghaowang@shu.edu.cn), Young-Kyun Kwon (ykkwon@khu.ac.kr), and Min-Cherl Jung (jung.mincherl.fp@u.tsukuba.ac.jp)

Figure S1. The THz spectra transmitting through the sample B and its reference in (a) time-, (b) frequency-domain, and (c) the transmission spectrum of each sample. (d) The THz-wave absorption property of the protection layer, PTAA polymer. Its transmission from 0.5 to 3.0 THz shows almost 98 % and there is no significant THz-wave absorption.

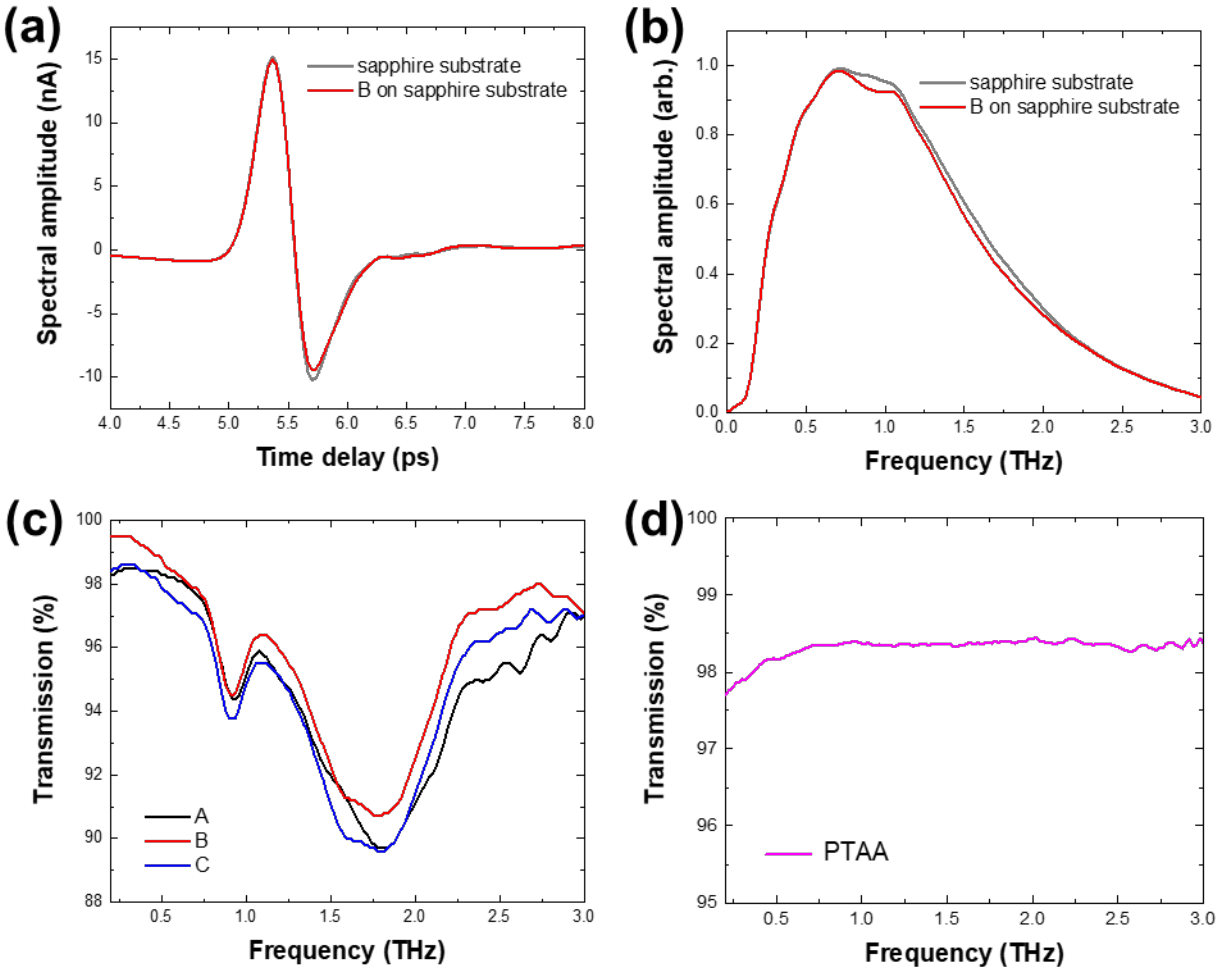

Figure S2. The C, N, and O 1*s* core-level spectra for the A, B, and C samples. The binding energies of C and O 1*s* show the typical physi-absorbed states that are due to the sample transfer from the N_2 glovebox to the vacuum chamber. There is no significant chemical state bonded to the $CsPbI_3$ thin films.

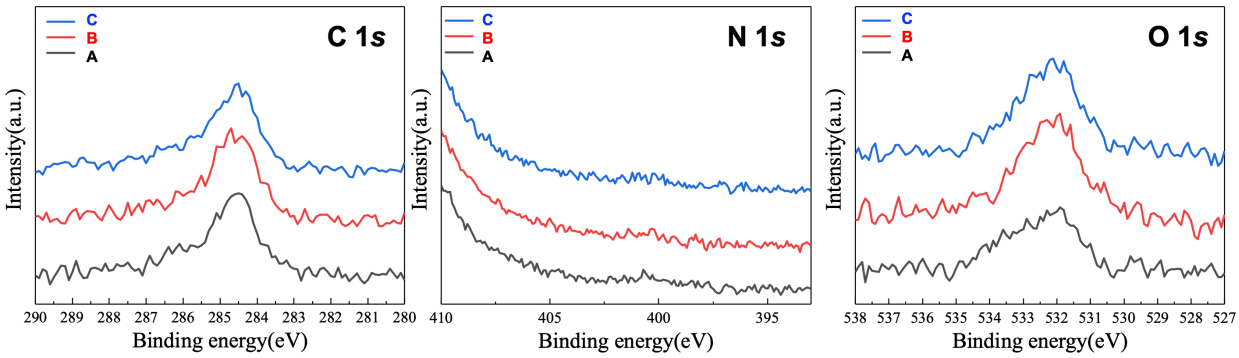

Figure S3. After the self-degradation, we confirmed all samples become δ-$CsPbI_3$ with PbI_2.

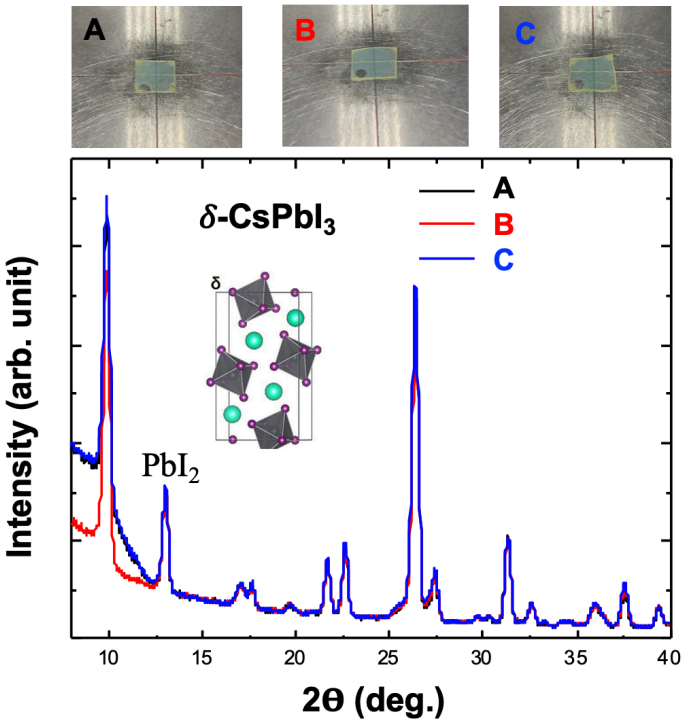

Figure S4. (a) THz-wave absorption properties of the A, B, and C samples with δ-$CsPbI_3$. (b-d) Conductivities and peak-fitting curves for the resonant phonon mode of A, B, and C samples.

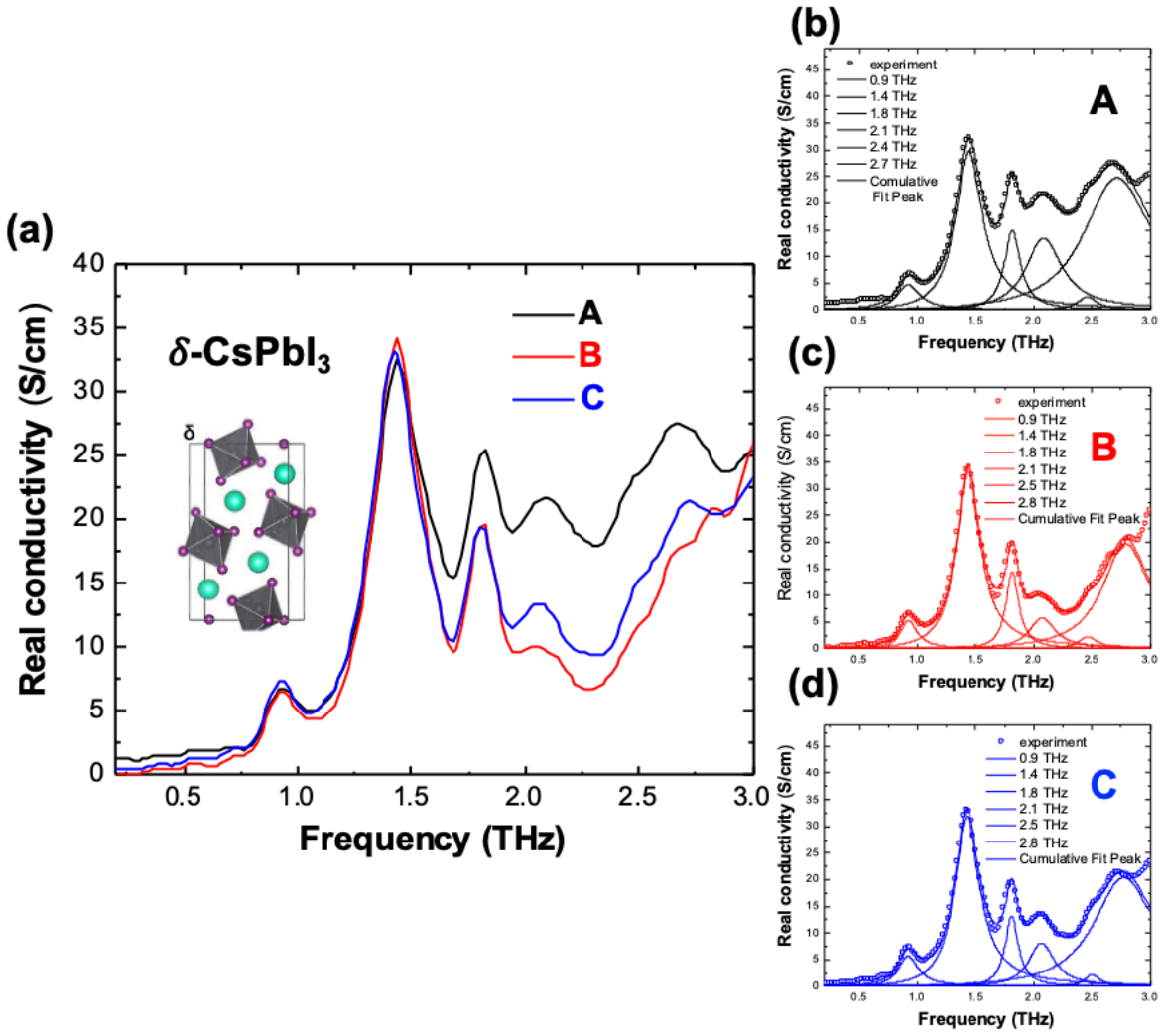

Figure S5. (a) Phonon band structure and (b) calculated THz absorption spectrum of bulk δ-$CsPbI_3$. (Black solid line) The THz absorption spectrum of γ-$CsPbI_3$ was also represented as a gray solid line for the comparison. (a) and (b) were calculated based on the theoretical equilibrium structure of δ-$CsPbI_3$ with equilibrium lattice constants of a = 4.753 Å, b = 10.415 Å and c = 17.676 Å. Blue arrows highlight strong absorption peaks of δ-$CsPbI_3$ that were described in Fig. S4.

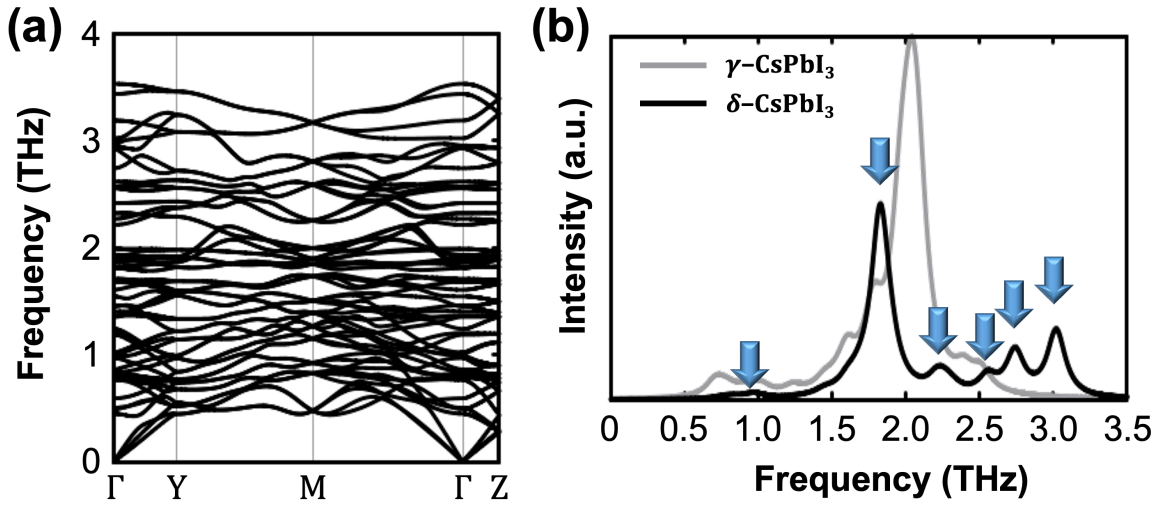

Figure S6. (a-f) Real-space visualization of phonon vibration modes of δ-$CsPbI_3$ at 0.96, 1.82, 2.27, 2.31, 2.55, and 3.02 THz, respectively. Grey, purple, and cyan balls indicate Pb, I, and Cs atoms and the red, blue, and brown arrows show their corresponding real-space displacement vectors, respectively.

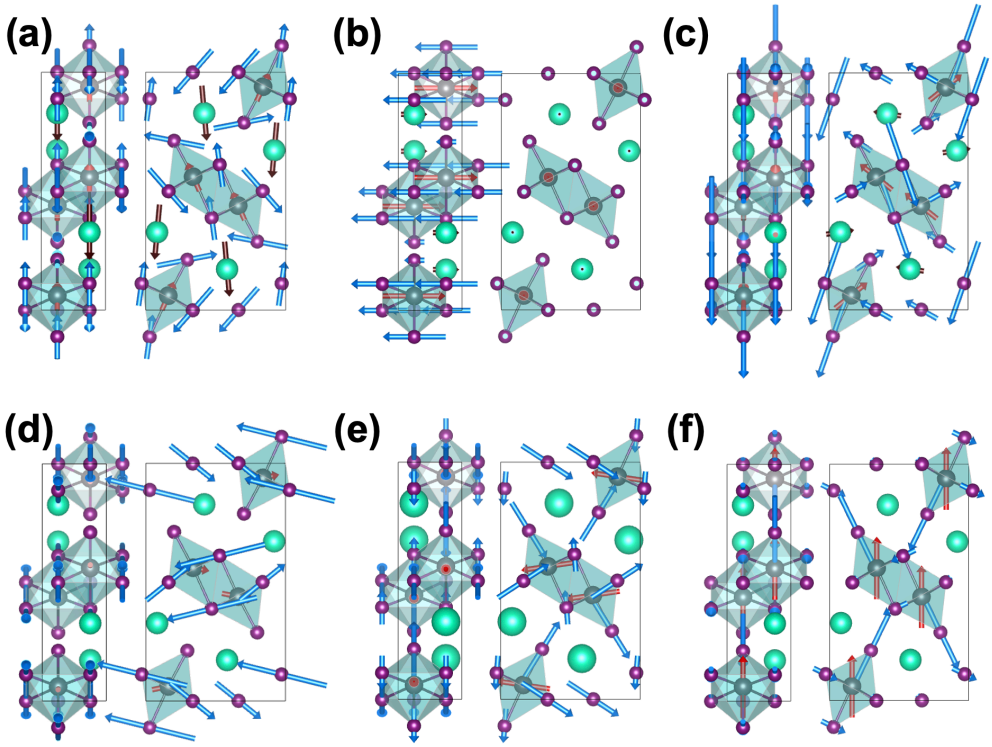

Table S1. Lorentzian parameters to describe THz conductivity of the A, B, and C samples with γ-$CsPbI_3$.

Sample	$\boldsymbol{\omega_{0j}/2\pi}$ **[THz]**	$\boldsymbol{\Omega_j/2\pi}$ **[THz]**	$\boldsymbol{\gamma_j/2\pi}$ **[THz]**
A	0.9	2.5	0.2
	1.5	4.8	0.7
	1.9	5.3	0.6
	2.1	1.2	0.2
	2.6	3.2	0.8
B	0.9	3.0	0.3
	1.5	4.0	0.5
	1.8	5.0	0.5
	2.0	1.3	0.2
	2.6	1.0	0.3
C	0.9	2.9	0.3
	1.5	4.2	0.5
	1.8	5.0	0.5
	2.1	1.3	0.2
	2.6	1.5	0.4

Table S2. Lorentzian parameters to describe THz conductivity of the A, B, and C samples with δ-$CsPbI_3$.

Sample	$\omega_{0j}/2\pi$ **[THz]**	$\Omega_j/2\pi$ **[THz]**	$\gamma_j/2\pi$ **[THz]**
A	0.9	1.4	0.2
	1.4	3.9	0.3
	1.8	2.1	0.2
	2.1	3.0	0.4
	2.5	0.9	0.2
	2.7	5.6	0.7
B	0.9	1.3	0.2
	1.4	3.8	0.2
	1.8	1.9	0.1
	2.1	1.7	0.3
	2.5	0.9	0.2
	2.8	4.2	0.5
C	0.9	1.5	0.2
	1.4	3.8	0.3
	1.8	1.8	0.1
	2.1	2.0	0.3
	2.5	0.8	0.2
	2.8	4.9	0.6